

# CO Oxidation on Palladium. 1. A Combined Kinetic-Infrared Reflection Absorption Spectroscopic Study of Pd(100)

János Szanyi<sup>1</sup> and D. Wayne Goodman\*

Department of Chemistry, Texas A&M University, College Station, Texas 77843

Received: September 9, 1993; In Final Form: December 9, 1993<sup>o</sup>

DTIC  
ELECTE  
SEP 14 1994  
B

94-29688



78

The oxidation of carbon monoxide on a Pd(100) single-crystal catalyst was studied using an elevated-pressure IR cell/ultrahigh vacuum surface analysis system. The kinetics of the reaction was followed by monitoring the total pressure change during the course of the reaction. Simultaneously, the surface concentration of adsorbed CO was measured using IR reflection absorption spectroscopy. An activation energy of  $29.4 \pm 0.3$  kcal/mol was found between 500 and 575 K at a total pressure of 1.50 Torr and  $\text{CO}/\text{O}_2 = 2$ . The IR data obtained under reaction conditions show the CO coverage to vary between 0.45 and 0.55 monolayers (ML). For this coverage regime, the CO heat of adsorption was determined to be  $29 \pm 2$  kcal/mol, corresponding closely to the apparent activation energy. Between 0.5 and 10.0 Torr, negative first-order CO and positive first-order oxygen pressure dependencies were measured<sup>1</sup>, yielding a zero-order total pressure dependence of the reaction rate. No change in CO coverage was observed with a change in the oxygen pressure, while the CO coverage increased from 0.50 ML at  $P_{\text{CO}} = 0.50$  Torr to 0.55 ML at  $P_{\text{CO}} = 8.0$  Torr.

DISTRIBUTION STATEMENT A

Approved for public release  
Distribution Unlimited

## Introduction

Because of its importance in automotive and industrial pollution control, the oxidation of carbon monoxide is one of the most extensively studied reactions on supported<sup>1-9</sup> and single-crystal (Pt, Pd, Rh, and Ru) catalysts.<sup>9-22</sup> Besides its practical importance, CO oxidation is an excellent example of a relatively simple heterogeneous catalytic reaction suitable for study over a wide range of reaction conditions, from ultrahigh vacuum to elevated pressures. From the extensive studies of this reaction over a variety of catalysts, some general conclusions can be drawn about the mechanism of CO oxidation. The reaction, in general, follows a Langmuir-Hinshelwood mechanism in that the reaction takes place between chemisorbed CO and dissociatively adsorbed oxygen atoms. Since the adsorption of CO occurs preferentially to oxygen, the catalyst surface is covered predominantly by CO, resulting in a CO desorption-limited rate under typical reaction conditions. This dominance of the surface by CO leads to the rate being negative order with respect to the CO partial pressure. For the oxygen partial pressure, a positive order is found. The rate, therefore, is essentially zero order with respect to the total pressure.

The oxidation of carbon monoxide is generally considered as the prototypical structure insensitive reaction.<sup>10,19</sup> Because CO desorption limits the reaction, the apparent activation energy for CO oxidation on a particular metal has been found to track the CO heat of adsorption on that metal. It is noteworthy, however, that for certain metals the CO heat of adsorption is known to be structure sensitive. For example, on the low-index planes of Pd [(100), (110), and (111)] the CO heats of adsorption vary significantly with coverage, particularly at the high-coverage limit.<sup>23-27</sup> Indeed, recent studies of CO oxidation on Pd(100), Pd(110), and Pd(111) indicate a subtle structure sensitivity for this reaction.<sup>9</sup>

Infrared reflection absorption spectroscopy (IRAS) has been shown to be an ideal tool for studying metal catalysts under working conditions at elevated pressures.<sup>28-32</sup> In this paper we report results of a study of carbon monoxide oxidation on a Pd-(100) catalyst at elevated pressures using a combined IRAS/kinetic approach. The main goal of this investigation and that

described in the following paper is to demonstrate a correspondence between the CO heat of adsorption and the apparent activation energy for CO oxidation on a Pd catalyst under a variety of conditions, particularly those that yield CO coverages near saturation. These results also address issues relevant to the degree and the nature of structure sensitivity of CO oxidation on Pd catalysts.

## Experimental Section

The experiments were carried out in a combined elevated-pressure IR cell/UHV surface analysis system described in detail elsewhere.<sup>33,34</sup> The UHV chamber is equipped with the basic surface analytical techniques of Auger electron spectroscopy (AES), low-energy electron diffraction (LEED), and temperature-programmed desorption (TPD). The elevated-pressure IR cell, equipped with two  $\text{CaF}_2$  windows, is connected to the UHV chamber via a double-differentially pumped sliding seal.<sup>34</sup> This arrangement facilitates elevated-pressure adsorption and kinetic studies in the pressure range of  $10^{-4}$ – $10^1$  Torr. The pressure in the IR cell was monitored with a nude ionization gauge in the pressure range of  $1 \times 10^{-2}$ – $1 \times 10^{-3}$  Torr and with a 10-Torr Baratron gauge at pressures  $> 1 \times 10^{-3}$  Torr.

The IRAS experiments were carried out using a slightly modified Cygnus 100 spectrometer equipped with a mercury cadmium telluride (MCT) detector. The CO adsorption spectra were obtained with 512 scans in the single-reflection mode with  $8\text{-cm}^{-1}$  resolution. In the kinetic studies, in order to shorten the spectral acquisition time, 16 scans with  $16\text{-cm}^{-1}$  resolution were used, reducing the collection time for each spectrum to 8 s. The catalytic experiments were carried out in the batch mode, and the reaction kinetics were followed by monitoring the total pressure change in the reaction cell.

The Pd(100) crystal was mounted on tantalum leads and was heated resistively. The crystal temperatures was monitored by a W-5%Re/W-26%Re thermocouple spotwelded to the edge of the crystal. The sample manipulator also allowed cooling of the sample to 90 K. The sample cleaning procedure was that discussed in ref 35, followed by an anneal to 1200 K. AES and LEED were utilized to verify sample cleanliness and the long range order of the crystal, respectively.

Research purity ( $> 99.999\%$ , Matheson) CO and  $\text{O}_2$  were used; CO was further purified by storing at liquid nitrogen temperatures throughout the study to ensure the removal of any transition-

\* To whom correspondence should be addressed.

<sup>1</sup> Present address: Los Alamos National Laboratory, CLS-1, MS J565, Los Alamos, NM 87545.

<sup>o</sup> Abstract published in *Advance ACS Abstracts*, February 15, 1994.

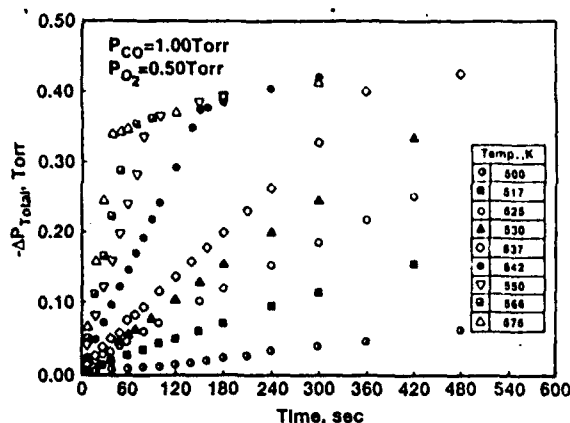


Figure 1. Total pressure change during the oxidation of carbon monoxide on Pd(100) as a function of reaction time.  $P_{\text{CO}} = 1.00$  Torr;  $P_{\text{O}_2} = 0.50$  Torr.

metal (Ni, Fe) carbonyl impurities; oxygen was used as received. CO-O<sub>2</sub> gas mixtures with the desired ratios were prepared in the reaction cell prior to the catalytic measurements.

### Results and Discussion

The effect of reaction temperature on the CO<sub>2</sub> formation rate was determined in the temperature range of 500–575 K using a CO/O<sub>2</sub> = 2 reactant gas mixture at a total pressure of 1.5 Torr. The total pressure change as a function of reaction time is displayed in Figure 1. At low reaction temperatures (500–530 K), the total pressure changes linearly with reaction time over the entire reaction period. For reaction temperatures >530 K and at a particular CO conversion, a sharp break in the data is evident. Subsequent to this break, the total pressure changes much more slowly relative to the initial portion of the reaction. The higher the reaction temperature, the lower the CO conversion corresponding to the break in the data.

Since the catalyst surface is predominantly covered by CO, the overall rate-determining step is the desorption of CO, a process that frees adsorption sites for the adsorption of oxygen. In the low CO conversion regime, this mechanism is operative and an increase in the reaction rate with increasing temperature is observed. The breaks in the data of the total pressure change versus reaction time represent points at which the conversion of CO is sufficient to reduce its partial pressure below the critical CO-limiting coverage at that particular temperature. Further reaction leads to a further reduction in the CO partial pressure (and coverage), yielding a steadily decreasing reaction rate. At sufficiently high CO conversion, the rate is essentially independent of temperature, reflecting the compensating effect of the reduced CO coverage on the overall reaction rate. IRAS confirms this explanation in that, subsequent to the breaks in the data of Figure 1, no CO was detected on the surface.

From the slopes of these data, initial CO<sub>2</sub> formation rates can be extracted. Specific CO<sub>2</sub> formation rates as a function of reaction temperature are shown in Figure 2 in Arrhenius form. From the slope of this plot an apparent activation energy of  $24.6 \pm 0.3$  kcal/mol is derived, a value approximately 2 kcal/mol higher than that reported by Logan et al. for this catalyst.<sup>16</sup>

To establish a correlation between the CO heat of adsorption and the apparent activation energy for the CO oxidation reaction, the adsorption of CO was studied over the pressure and temperature ranges of  $10^{-7}$ – $10.0$  Torr and 90–1000 K, respectively. The results of this adsorption study are discussed in detail elsewhere<sup>36</sup> and can be used to determine the CO heat of adsorption on Pd(100) as a function of coverage. In Figure 3 the integrated IR intensities are plotted as a function of adsorption temperature for some representative CO pressures. The integrated IR intensities increase monotonically with increasing CO coverage

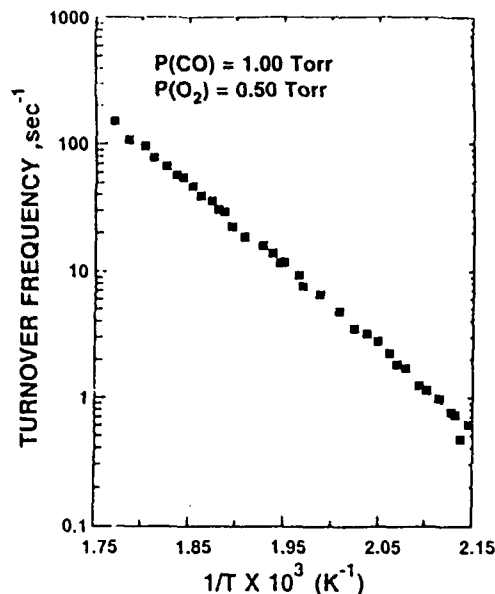


Figure 2. Specific CO<sub>2</sub> formation rates on Pd(100) as a function of temperature in Arrhenius form.  $P_{\text{CO}} = 1.00$  Torr;  $P_{\text{O}_2} = 0.50$  Torr.

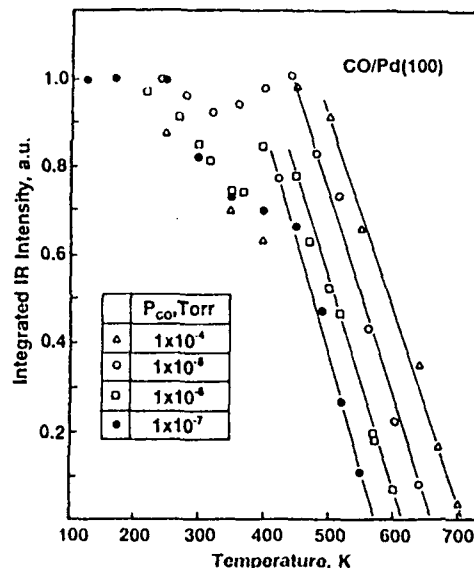


Figure 3. Representative CO adsorption isobars on Pd(100) at pressures of  $1 \times 10^{-7}$ ,  $1 \times 10^{-6}$ ,  $1 \times 10^{-5}$ , and  $1 \times 10^{-4}$  Torr.

(decreasing adsorption temperature) up to an integrated intensity of  $\sim 0.8$ , at which point discontinuities are apparent in the plots. The points of discontinuity in the plots correspond to a CO coverage of  $\sim 0.5$  ML, that CO coverage at which a commensurate-incommensurate CO phase transition is known to occur.<sup>37</sup> Above 0.5 ML coverage several compressed CO overlayer structures have been noted for Pd(100).<sup>37</sup> This compression of the CO results in a strongly repulsive interaction among neighboring adsorbed CO molecules, yielding a dramatic change in the dynamic dipole moments of the adsorbed CO molecules. This, in turn, results in the altered IR absorption cross sections.<sup>37</sup> These changes in the IR absorption cross sections give rise to the attenuation of the integrated IR intensities at CO coverages above 0.5 ML. An increase in the CO coverage significantly above 0.5 ML leads to a further increase in the IR intensity up to a saturation coverage of 0.8 ML. Because of the uncertainty in the coverage versus IR intensity relationship above a CO coverage of 0.5 ML, only those data corresponding to a CO coverage  $< 0.5$  ML will be discussed.

The results here conflict with the previous data of Ortega et al.,<sup>38</sup> who noted that the integrated IR intensity increased linearly

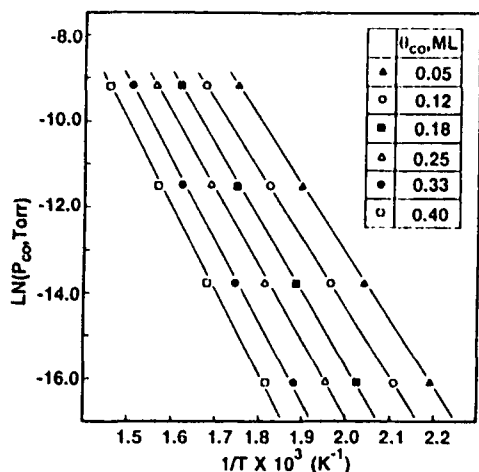


Figure 4. Representative isosteric plots of  $\ln(P_{\text{CO}})$  versus  $1/T$  for Pd(100).

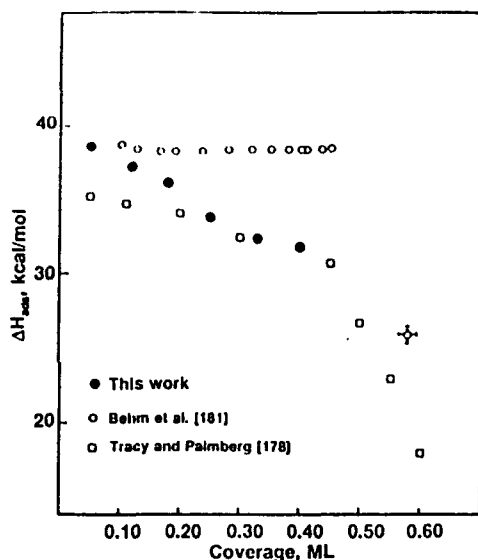


Figure 5. Isosteric heats of adsorption of CO on Pd(100) as a function of CO coverage. (For comparison, data obtained by Tracy et al.<sup>23</sup> and Behm et al.<sup>40</sup> are also displayed.)

up to 0.5 ML and then remained constant. However, a careful examination of their data in Figure 9 of ref 38 reveals that there is indeed a decrease in the integrated IR intensity at the point of the CO phase transition, followed by an increase in the integrated intensity at higher CO coverages. A similar behavior has been observed for the CO/Pd(111) system (following paper) where two phase transitions occur.<sup>39</sup> These results suggest that discontinuities in the adsorption isobars likely will be evident in those adsorption systems in which such phase transitions take place.

From the adsorption isobars of Figure 3, isosteric plots of  $\ln(P_{\text{CO}})$  versus  $1/T$  can be constructed for various CO coverages. The single assumption made is that identical integrated IR intensities correspond to identical CO coverages. Representative isosteric plots for the CO/Pd(100) system are shown in Figure 4. In previous studies,<sup>36</sup> the adsorption of CO on Pd(100) has been observed to be completely reversible over the entire coverage regime; therefore, the Clausius-Clapeyron equation ( $d(\ln P)/d(1/T) = -E/R$ ) can be used to estimate the CO heat of adsorption. The isosteric heats of adsorption of CO as a function of coverage are shown in Figure 5. Uncertainties in determining the integrated IR intensities lead to a  $\pm 2$  kcal/mol error. For comparison, data obtained by Tracy and Palmberg<sup>23</sup> and Behm et al.<sup>40</sup> are included. The Tracy and Palmberg data<sup>23</sup> were derived using work function measurements and LEED analysis, whereas

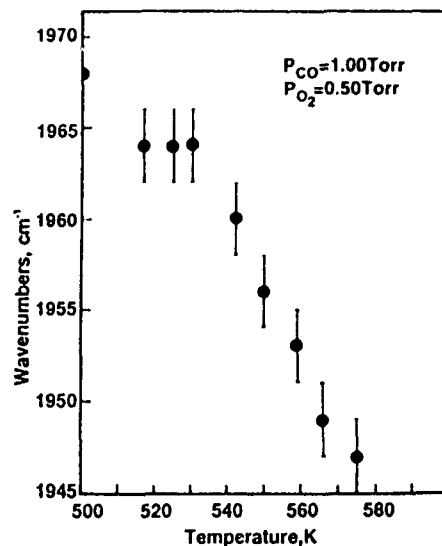


Figure 6. Stretching frequency of adsorbed CO on Pd(100) as a function of reaction temperature.  $P_{\text{CO}} = 1.00$  Torr;  $P_{\text{O}_2} = 0.50$  Torr.

Behm et al.<sup>40</sup> determined the coverage-dependent isosteric heats of adsorption utilizing work function data. The agreement among the results of these three studies at low CO coverages is reasonably good. In this study an isosteric CO heat of adsorption of 38.6 kcal/mol was determined at a coverage of 0.05 ML. The CO heat of adsorption decreased monotonically with increasing coverage. The initial heat of adsorption is identical, within the limit of experimental error, to that found by Behm et al.<sup>40</sup> but approximately 3 kcal/mol higher than that determined by Tracy and Palmberg.<sup>23</sup> However, as the coverage increases, the CO heats of adsorption obtained here follow very closely the values obtained by Tracy and Palmberg.<sup>23</sup> Practically no decrease in the CO heat of adsorption was seen by Behm et al.<sup>40</sup> over a very wide CO coverage region of 0.00–0.45 ML. It is noteworthy that in a previous study<sup>36</sup> the IR frequency of adsorbed CO has been shown to significantly blue-shift with increasing coverage in the range of 0.00–0.45 ML, consistent with a weakening of the Pd–CO bond and to a reduction in the CO heat of adsorption.

To establish a direct correlation between the apparent activation energy for CO oxidation and the CO heat of adsorption determined from the IR study, the surface coverage of CO was estimated under reaction conditions using IRAS. In the initial, constant reaction rate region, IR spectra of adsorbed CO were acquired at each reaction temperature. The C–O stretching frequency under steady-state reaction conditions as a function of reaction temperature is shown in Figure 6. The C–O stretching frequency of adsorbed CO decreases monotonically with increasing reaction temperature, consistent with a reduction in the CO coverage with increasing reaction temperature. The C–O stretching frequency decreases from 1968 to 1947  $\text{cm}^{-1}$  as the reaction temperature increases from 500 to 575 K. Since the oxygen coverage under these conditions is insignificant, these stretching frequencies can be used to estimate the surface coverages of CO on the basis of the measured stretching frequency–coverage calibration curve.<sup>36</sup> The frequency range 1968–1947  $\text{cm}^{-1}$  suggests a CO coverage range of 0.45–0.55 ML, corresponding to a CO overlayer structure characterized by a  $c(2\sqrt{2} \times \sqrt{2})R45^\circ$  LEED structure. The CO heat of adsorption within this coverage range is approximately 29 kcal/mol, a value very close to the  $29.4 \pm 0.3$  kcal/mol apparent activation energy determined for the CO oxidation reaction in the 500–575 K temperature range.

Logan et al.<sup>16</sup> have studied the oxidation of CO on Pd(100) under identical reaction conditions and have drawn very similar conclusions. However, in their study no direct spectroscopic evidence was available to determine the precise CO coverages under reaction conditions. These authors assumed that the CO

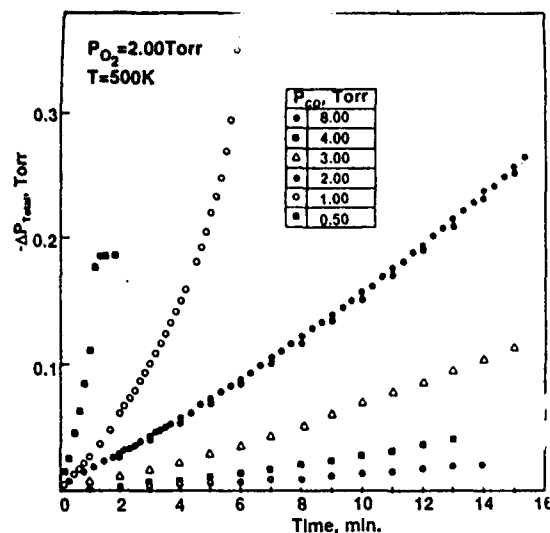


Figure 7. Total pressure change during the oxidation of CO on Pd(100) as a function of reaction time at CO partial pressures of 8.00, 4.00, 3.00, 2.00, 1.00, and 0.50 Torr.  $P_{O_2} = 2.00$  Torr;  $T = 500$  K.

coverage on Pd(100) at  $P_{CO} = 1.00$  Torr was approximately 0.5 ML, yielding very similar heats of adsorption and apparent activation energies. Logan et al. also studied the effect of the total pressure on the kinetics of CO oxidation using two different total pressures while maintaining a constant CO/O<sub>2</sub> = 2 reactant gas mixture. Under the reaction conditions identical to those employed here, these authors found an apparent activation energy of 27 kcal/mol. With an increase in the total pressure from 1.5 to 24 Torr, Logan et al. observed a decrease in the activation energies from 27 to 21 kcal/mol. The difference in the apparent activation energies was explained to arise from different CO coverages under the two reaction conditions, resulting in different CO heats of adsorption. They concluded that the CO coverage at  $P_{CO} = 1.00$  Torr was near 0.5 ML and that at  $P_{CO} = 16.0$  Torr near 0.55 ML. This small increase in CO coverage is sufficient to lead to a decrease of 6 kcal/mol in the CO heat of adsorption. The results of our IR experiments show that this is indeed the case. The IR spectrum of adsorbed CO at  $P_{CO} = 10.0$  Torr and  $T = 525$  K yields a C–O stretching frequency of 1975 cm<sup>-1</sup>, which corresponds to a CO coverage of slightly above 0.55 ML. The corresponding heat of CO adsorption at this coverage is 20 kcal/mol, which agrees well with the 21 kcal/mol activation energy for CO oxidation on Pd(100) reported by Logan et al.<sup>16</sup> at  $P_{CO} = 16.0$  Torr.

The reaction rate dependences on the partial pressures of CO and O<sub>2</sub> were also studied and are shown in Figures 7 and 8. In both cases the total pressure changes were monitored as a function of reaction time for different reactant mixtures at 500 K. The total pressure changes linearly with reaction time for stoichiometric CO/O<sub>2</sub> mixtures throughout the reaction period. A slight increase in the oxygen partial pressure above stoichiometry results in a deviation of the rate from linearity. This increasing rate with reaction time reflects the steadily increasing O<sub>2</sub>/CO ratio with time for these mixtures. A break in each plot of total pressure change versus reaction time occurs at CO conversions that yield approximately the same residual CO partial pressure. As discussed above, this break corresponds to that point at which the CO partial pressure falls below that required to achieve a critical CO-limiting coverage at 500 K ( $\sim 0.2$  Torr). For  $P_{CO} < 2.0$  Torr in Figure 7, breaks in the plots occur at points corresponding to  $P_{CO} \sim 0.2$  Torr ( $\Delta P_{\text{total}} \sim 0.18$  Torr for  $P_{CO} = 0.50$  Torr, and  $\Delta P_{\text{total}} \sim 0.36$  Torr for  $P_{CO} = 1.00$  Torr). The total pressure changes linearly with reaction time during the entire reaction for CO/O<sub>2</sub> > 2 since the partial pressure of CO for these mixtures never falls below the critical CO-limiting value of  $\sim 0.2$  Torr. IRAS inspection of the surface subsequent to the breaks

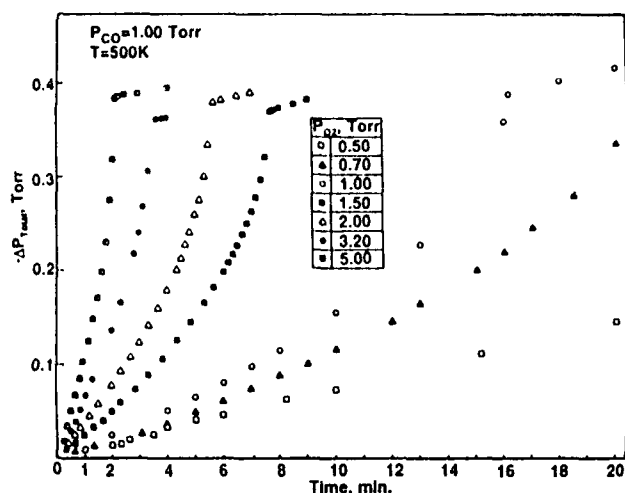


Figure 8. Total pressure change during the oxidation of CO on Pd(100) as a function of reaction time at oxygen partial pressures of 5.00, 3.20, 2.00, 1.50, 1.00, 0.70, and 0.50 Torr.  $P_{CO} = 1.00$  Torr;  $T = 500$  K.

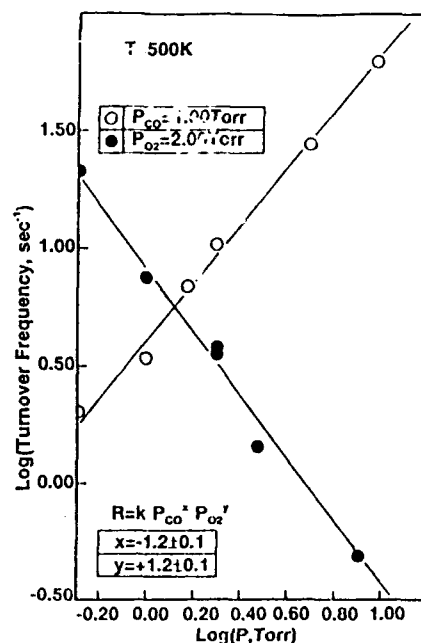


Figure 9. Specific CO<sub>2</sub> formation rate on Pd(100) as a function of oxygen (O) and CO (●) partial pressures.  $T = 500$  K.

in Figure 7, as noted for the breaks in the data of Figure 1, shows no detectable CO on the surface.

From the slopes of these plots, the initial reaction rates can be determined for the CO and oxygen partial pressure dependencies. These results are shown in Figure 9, in which the specific CO<sub>2</sub> formation rates are plotted versus the partial pressures of the reactants in logarithmic forms. The slopes of these plots define the order of the reaction rate with respect to the reactant partial pressure. With respect to the oxygen partial pressure, this value is 1.2; with respect to the CO pressure, the dependency is -1.2. Both are in excellent agreement with the orders determined by Logan et al.<sup>16</sup> The combined dependencies of O<sub>2</sub> and CO suggest that the overall reaction rate is zero order in total pressure within the limited pressure range of this study.

In both the CO and O<sub>2</sub> partial pressure studies, IRAS was used to follow the surface coverage of CO during reaction. No change in the stretching frequency of adsorbed CO (1964 cm<sup>-1</sup>) was observed while the oxygen pressure was changed over the range 0.5–8.0 Torr; the 1964-cm<sup>-1</sup> C–O stretching frequency corresponds to a CO coverage of  $\sim 0.5$  ML. Although no change in CO coverage was apparent, the reaction rate increased (first-

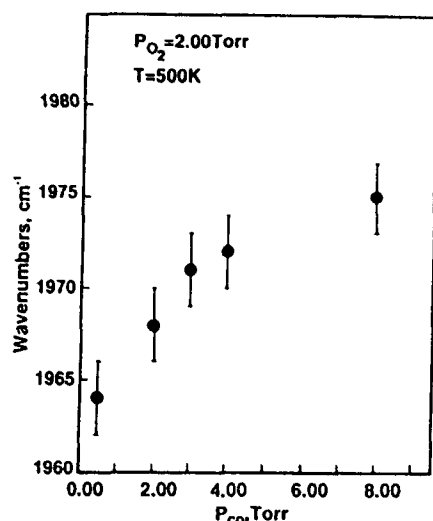


Figure 10. Stretching frequency of adsorbed CO on Pd(100) as a function of CO partial pressure.  $P_{O_2} = 2.00$  Torr;  $T = 500$  K.

order) with  $P_{O_2}$ . The increasing oxygen pressure, however, does not measurably alter the composition of the adsorbed surface layer. That is, even in the  $O_2$  rich CO/ $O_2$  mixtures studied, CO adsorbs preferentially on the Pd(100) surface. That the CO adsorption is unaffected by  $O_2$  adsorption is apparent in Figure 8 in that the breaks in the data for  $P_{O_2} \geq 1.00$  Torr occur at identical partial pressures of CO ( $\sim 0.2$  Torr). This behavior reflects the invariance of the CO adsorption energy for each of these reaction conditions.

In contrast to the oxygen partial pressure study, a change in the CO partial pressure produced a shift in the C–O stretching frequency, even in the very limited CO partial pressure range of 0.5–8.0 Torr. Figure 10 shows the C–O stretching frequency as a function of the CO partial pressure. From these frequencies, CO surface coverages under reaction conditions can be estimated. For example, the surface CO coverage at  $P_{CO} = 0.50$  Torr is approximately 0.50; at  $P_{CO} = 8.0$  Torr the CO coverage is significantly greater than 0.5 ML. This means that an increase in CO pressure from 0.5 to 8.0 Torr is sufficient to promote the CO phase transition, yielding a compressed CO overlayer structure.

The results of our elevated-pressure CO adsorption IR experiments are useful in explaining the CO and  $O_2$  partial pressure dependencies observed by Logan et al.<sup>22</sup> These authors observed a decrease in the order of oxygen partial pressure dependency upon an increase in the CO partial pressure from 1 to 16 Torr. First-order reaction rate dependence on oxygen partial pressure was observed at CO coverages below 0.5 ML, e.g.  $P_{CO} = 1.00$  Torr. However, at  $P_{CO} = 16.0$  Torr the CO coverage is higher than 0.5 ML, and thus the CO adlayer is compressed. Accordingly, the overall reaction rate is not first order with respect to the oxygen pressure but, rather, significantly less than one. Similarly, at low CO pressures, i.e.  $\theta_{CO} < 0.50$  ML, the reaction rate with respect to the CO pressure is negative first order in CO partial pressure. Upon increasing the CO pressure above a critical value, the Pd(100) surface is covered by more than half of a monolayer of CO. A further increase in the CO pressure does not decrease the overall reaction rate as dramatically as seen for the low CO pressures.

This work shows clearly that the apparent activation energy of the CO oxidation reaction on Pd(100) follows closely the CO adsorption energy, a conclusion supported by the findings of Logan et al.<sup>22</sup> That the CO adsorption energy varies with coverage and, to a degree, the Pd crystal facet raises the issue of the structure sensitivity of the CO oxidation on Pd catalysts. The CO heat of adsorption as a function of CO coverage is well documented for the three low-index Pd crystal faces.<sup>9,29–33</sup> The CO heats of

adsorption at low coverages on these three surfaces are very close and fall in the range of 35–40 kcal/mol. Under the conditions typically used in CO oxidation studies, low CO coverages are not realized; low coverages are found only at very high reaction temperatures or at very low CO/ $O_2$  ratios. However, the CO heats of adsorption for the (111), (110), and (100) faces of Pd change characteristically with CO coverage. There are significant differences in the CO heats of adsorption on the different low-index planes of Pd crystals in the CO coverage range of 0.4–0.6 ML, a coverage that is realized at typical CO oxidation conditions. For example, at  $\theta_{CO} = 0.50$  the CO heats of adsorption are 17,<sup>33</sup> 33,<sup>32</sup> and 29 kcal/mol<sup>29</sup> for the (111), (110), and (100) faces of Pd, respectively. The results of this study suggest that, as far as the CO heat of adsorption is structure sensitive, the oxidation of CO should be structure sensitive as well. The apparent structure insensitivity of the CO oxidation reaction on Pd catalysts reported to date is likely due to the varying CO coverages realized for different crystal orientations at similar reaction conditions. Our adsorption<sup>29,36</sup> and kinetic<sup>9</sup> studies have shown that the CO coverages on different Pd crystal faces are significantly different under identical experimental conditions. These variations in the CO coverages, and the accompanying differences in the heats of adsorption of CO, can mask any intrinsic structure sensitivity. Experiments in which the CO oxidation reaction is carried out under conditions that produce identical steady-state CO surface coverages on different Pd surfaces could verify the structure-sensitive nature of the reaction.

### Summary

(1) An apparent activation energy of  $29.4 \pm 0.3$  kcal/mol is found for the oxidation of carbon monoxide on Pd(100) at a total pressure of 1.5 Torr and CO/ $O_2 = 2$  in the temperature range of 500–575 K. In situ IRAS measurements show that the CO coverage at these reaction conditions is 0.45–0.55 ML, yielding a CO heat of adsorption of  $29 \pm 2$  kcal/mol.

(2) Positive first-order oxygen and negative first-order CO partial pressure dependencies of the overall reaction rate are seen in the pressure range of 0.5–10.0 Torr.

(3) In the very limited CO partial pressure range of 0.5–8.0 Torr, the CO coverage increases from 0.50 to 0.55 ML. This coverage region extends over the entire range at which the CO overlayer undergoes a phase transition to a compressed CO adlayer. Formation of the compressed layer significantly lowers the adsorption energy of CO.

(4) The correlations found between the heats of adsorption of CO and the apparent activation energies for CO oxidation on Pd(100) suggest that the oxidation of carbon monoxide on Pd is a structure-sensitive reaction to the extent that CO adsorption is structure sensitive.

**Acknowledgment.** We acknowledge with pleasure the support of this work by the Department of Energy, Office of Basic Energy Sciences, Division of Chemical Sciences.

### References and Notes

- Oh, S. H. *J. Catal.* **1990**, *124*, 477.
- Choi, K. I.; Vannice, M. A. *J. Catal.* **1991**, *127*, 465. Choi, K. I.; Vannice, M. A. *J. Catal.* **1991**, *127*, 489. Choi, K. I.; Vannice, M. A. *J. Catal.* **1991**, *131*, 22. Choi, K. I.; Vannice, M. A. *J. Catal.* **1991**, *131*, 36. Choi, K. I.; Vannice, M. A. *J. Catal.* **1991**, *131*, 1.
- Oh, S. H.; Eickel, C. C. *J. Catal.* **1991**, *128*, 526.
- Schlatter, J. C.; Taylor, K. C. *J. Catal.* **1972**, *49*, 42.
- Cant, N. W.; Hicks, P. C.; Lennon, B. S. *J. Catal.* **1978**, *54*, 372.
- Ladas, S.; Poppa, H.; Boudart, M. *Surf. Sci.* **1981**, *102*, 151.
- Oh, S. H.; Carpenter, J. C. *J. Catal.* **1983**, *80*, 472.
- Cant, N. W.; Angove, D. E. *J. Catal.* **1986**, *97*, 36.
- Xu, X.; Szanyi, J.; Xu, Q.; Goodman, D. W. *Catal. Today*, in press.
- Engel, T.; Ertl, G. *Adv. Catal.* **1978**, *28*, 1.
- Engel, T.; Ertl, G. *J. Chem. Phys.* **1978**, *69*(3), 1267.
- Steve, E. M.; Madix, R. J.; Brundle, C. R. *Surf. Sci.* **1984**, *146*, 155.
- Daniel, M.; White, J. M. *Int. J. Chem. Kinet.* **1985**, *17*, 413.

- (14) Swartz, S. B.; Schmidt, L. D.; Fisher, G. B. *J. Phys. Chem.* **1986**, *90*, 6194.  
 (15) Peden, C. H. F.; Houston, J. E. *J. Catal.* **1991**, *128*, 405.  
 (16) Logan, A. D.; Paffett, M. T. *J. Catal.* **1992**, *133*, 179.  
 (17) Peden, C. H. F.; Goodman, D. W. *J. Vac. Sci. Technol. A* **1985**, *3*(3), 1558.  
 (18) Oh, S. H.; Fisher, G. B.; Carpenter, J. E.; Goodman, D. W. *J. Catal.* **1986**, *100*, 360.  
 (19) Goodman, D. W.; Peden, C. H. F. *J. Phys. Chem.* **1986**, *90*, 4839.  
 (20) Peden, C. H. F.; Goodman, D. W.; Blair, B. S.; Berlowitz, P. J.; Fisher, G. B.; Oh, S. H. *J. Phys. Chem.* **1988**, *92*, 1563.  
 (21) Berlowitz, P. J.; Peden, C. H. F.; Goodman, D. W. *J. Phys. Chem.* **1988**, *92*, 5213.  
 (22) Leung, L.-W. H.; Goodman, D. W. *Catal. Lett.* **1990**, *5*, 353.  
 (23) Tracy, J. C.; Palmberg, P. W. *J. Chem. Phys.* **1969**, *51*, 4852.  
 (24) Tracy, J. C.; Palmberg, P. W. *Surf. Sci.* **1969**, *14*, 274.  
 (25) Bradshaw, A. M.; Hoffmann, F. M. *Surf. Sci.* **1978**, *72*, 513.  
 (26) Conrad, H.; Ertl, G.; Koch, J.; Latta, E. E. *Surf. Sci.* **1974**, *43*, 462.  
 (27) Gao, X.; Yates, J. T. *J. Chem. Phys.* **1989**, *90*(11), 6761.  
 (28) Truong, C. M.; Rodriguez, J. A.; Goodman, D. W. *Surf. Sci.* **1992**, *271*, L385.  
 (29) Kuhn, W. K.; Szanyi, J.; Goodman, D. W. *Surf. Sci.* **1992**, *274*, L611.  
 (30) Peden, C. H. F.; Goodman, D. W.; Weisel, M. D.; Hoffmann, F. M. *Surf. Sci.* **1991**, *253*, 44.  
 (31) Taylor, A. O.; Pritchard, J. J. *Chem. Soc. Faraday Trans.* **1990**, *86*, 2743.  
 (32) Peden, C. H. F.; Hoffmann, F. M. *Catal. Lett.* **1991**, *10*, 91.  
 (33) Leung, L.-W. H.; He, J.-W.; Goodman, D. W. *J. Chem. Phys.* **1990**, *93*, 8378.  
 (34) Campbell, R. A.; Goodman, D. W. *Rev. Sci. Instrum.* **1992**, *63*, 172.  
 (35) Grunze, M.; Ruppender, H.; Elshazly, O. *J. Vac. Sci. Technol. A* **1988**, *6*, 1266.  
 (36) Szanyi, J.; Kuhn, W. K.; Goodman, D. W. *J. Vac. Sci. Technol. A* **1993**, *11*, 1969.  
 (37) Brendt, W.; Bradshaw, A. M. *Surf. Sci.* **1992**, *279*, L165.  
 (38) Ortega, A.; Hoffmann, F. M.; Bradshaw, A. M. *Surf. Sci.* **1982**, *119*, 79.  
 (39) Szanyi, J.; Kuhn, W. K.; Goodman, D. W. *J. Phys. Chem.*, following paper.  
 (40) Behm, R. J.; Christmann, K.; Ertl, G.; Van Hove, M. A. *J. Chem. Phys.* **1980**, *73*, 2984.

Accession For	
NTIS GRA&I	<input type="checkbox"/>
DTIC TAB	<input type="checkbox"/>
Unannounced	<input type="checkbox"/>
Justification	
By	
Distribution	
Availability Codes	
Dist	Avail and/or Special
A	